

Letter to the Editor

The gamma-ray burst of 3 May 1991 observed by COMPTEL on board GRO

C. Winkler⁴, K. Bennett⁴, H. Bloemen², W. Collmar¹, A. Connors³, R. Diehl¹, A. van Dordrecht⁴, J.W. den Herder², W. Hermsen², M. Kippen³, L. Kuiper², G. Lichti¹, J. Lockwood³, M. McConnell³, D. Morris³, J. Ryan³, V. Schönfelder¹, G. Stacy³, H. Steinle¹, A. Strong¹, B. Swanenburg², B.G. Taylor⁴, M. Varendorff¹, and C. de Vries²

¹ Max-Planck Institut für Extraterrestrische Physik, D/W-8046 Garching, Germany

² Laboratory for Space Research Leiden, P.B. 9504, NL-2300 RA Leiden, The Netherlands

³ University of New Hampshire, Institute for the Studies of Earth, Oceans and Space, Durham NH 03824, USA

⁴ Astrophysics Division, Space Science Department of ESA/ESTEC, NL-2200 AG Noordwijk, The Netherlands

Received November 7, accepted November 19, 1991

Abstract. The Compton Gamma-Ray Observatory GRO was launched on April 5, 1991 carrying the imaging Compton telescope COMPTEL. Since its activation on April 25, 1991, COMPTEL has observed several gamma-ray bursts in its 1 sr field of view. The strongest of these bursts was observed on May 3, 1991. Event data over 0.8 MeV to 30 MeV as well as time resolved spectra over 0.1 MeV to 10 MeV have been recorded. *For the first time, a direct single-telescope MeV image of a cosmic gamma-ray burst has been produced.* The burst is located at (l,b) = (171.8°, 6.4°) with a statistical uncertainty (99% level) of about 2°. The systematic error is about 1° due to the location of the burst near the edge of the COMPTEL field-of-view. Spectral analysis indicates that GRB 910503 is a "classical" hard burst, with power-law emission up to several MeV, showing "hard-to-soft" spectral evolution in its lightcurve.

Key words: Gamma-ray bursts – COMPTEL – GRO

1. Introduction

The imaging Compton telescope COMPTEL is one of four instruments on board the Compton Gamma-Ray Observatory satellite (GRO), launched on space shuttle Atlantis on April 5, 1991 into a 450 km, 28.5° orbit. COMPTEL operates in the 0.8 MeV to 30 MeV range with a field of view of 1 steradian, an angular resolution of apx. 1° (1 σ), and an energy resolution of better than 10% FWHM. During its initial lifetime COMPTEL has observed many cosmic gamma-ray bursts in its field of view. In this paper we report on the observations of the strongest of these bursts so far, GRB 910503, including a direct image at MeV energies and first results from spectral analysis.

Send offprint requests to: C.Winkler

2. Instrument and operating modes

Gamma-ray bursts can be observed by COMPTEL using two independent operating modes, the "Double Scatter Mode" and the "Single Detector Mode". In the "Double Scatter Mode", which is the normal imaging mode, a gamma-ray photon is first Compton scattered in one of the 7 upper low-Z material detectors (D1 array, liquid scintillator NE 213A, total area 4188 cm²) followed by an interaction in a high-Z detector of the lower array (D2 array, 14 Na I cells, total area 8620 cm², see Fig.1 for illustration). The measured quantities per event

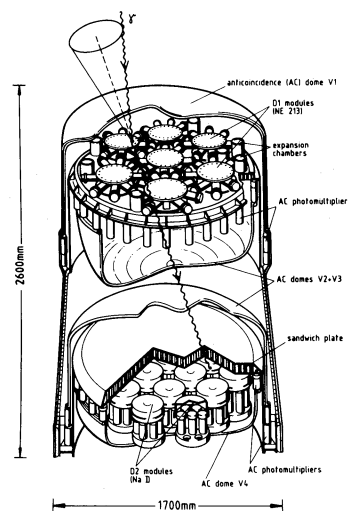


Fig. 1. Schematic view of COMPTEL

include the locations and energy deposits of these interactions in D1 and D2, the pulse shape of the interaction in the upper (D1) detector, the absolute time (125 μ s accuracy) of the event and the time - of - flight of the scattered photon from upper to lower detector. Measurement of the pulse shape in D1 allows rejection of neutron induced events, and a suitable window set on the time - of - flight permits rejection of most

of the background events (e.g. first scattered in D2 followed by an interaction in D1). The possible arrival directions for completely absorbed gamma events lie on a circle with radius ϕ around the direction of the scattered gamma-ray:

$$\cos(\phi) = 1 - \frac{mc^2}{E_2} + \frac{mc^2}{(E_1 + E_2)} \quad (1)$$

where mc^2 is the electron rest energy, E_1 and E_2 are the energy deposits of the gamma-ray in the upper and lower detector respectively (Fig. 1). The origin of emission can be located using event circles from different source gamma-rays. Events which are not completely absorbed in the NaI detector produce circles which do not intersect at the source position. A detailed description of the instrument and its imaging characteristics is given by Schönfelder et al. (1984).

The "Single Detector Mode" is described in detail by Winkler et al. (1986). Summarising, COMPTEL uses 2 of the lower 14 NaI detectors (see Fig. 1) to accumulate burst spectra upon receipt of a trigger signal from the Burst And Transient Source Experiment BATSE on board GRO. The detectors are, in principle, 4π sensitive. However, their on-axis field of view is largely obstructed by the upper D1 detector array. At larger zenith angles ($> 45^\circ$), obstruction is due to other GRO instruments, electronics boxes, spacecraft structure etc. The two detectors measure different energy regions: low range (apx. 0.1 MeV - 1.1 MeV, binwidth ~ 9.8 keV) and high range (apx. 1 MeV - 10 MeV, binwidth ~ 84.7 keV). In the absence of the BATSE trigger, background spectra (2 - 512 s telecommandable integration time) are accumulated and read out from both burst detectors. These data are used to investigate the total (instrumental + astrophysical) background before and after a burst event. After receipt of the BATSE burst trigger, 6 high resolution burst spectra (0.1 s to 25.6 s telecommandable integration time) are recorded. After the 6th spectrum a sequence of intermediate time resolution (tail) spectra (2 - 512 s telecommandable integration time) is accumulated and read out. After the last tail spectrum (maximum number = 255), the normal background mode is entered again. The configuration for the burst detector system during the initial phase of COMPTEL operation (which included the observation of GRB 910503) was: background mode 100 s integration (consecutive integration and read-out); six burst spectra each with 0.5 s integration time; 133 tail spectra, each with 6 s integration time.

3. Observational data and results

3.1. Time histories

On 3 May 1991 an outburst of celestial MeV gamma radiation was observed by COMPTEL. At that time, three out of 21 modules (D1-7, D2-1 and D2-5) were not operating while awaiting outgassing, resulting in 73% operational efficiency. A lightcurve of 0.8 - 30 MeV gamma events obtained in its normal imaging "Double Scatter Mode" is shown in Figure 2. This time history clearly demonstrates that GRB 910503 was a very strong source compared to normal event rate (~ 6 Hz), leading to a saturation of the event data buffers prior to data transmission. The initial rise (compare with Fig. 3) is visible. However, the rapid saturation of the buffer prevents acceptance of further events and results in the first gap. The end of this gap corresponds to the start of the next read-out period. The comparable amplitudes of the "peaks" is due to the fact that the

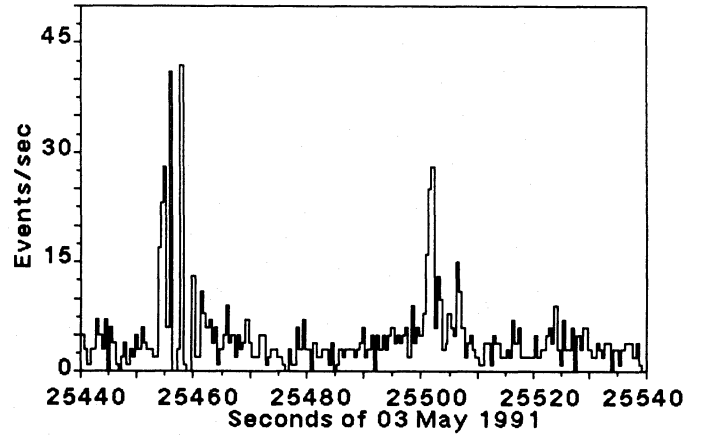


Fig. 2. GRB 910503: Lightcurve from COMPTEL imaging events. Data contain raw events without application of any selection criteria.

high event rate (> 23 Hz), re-saturates the buffer immediately after event read-out.

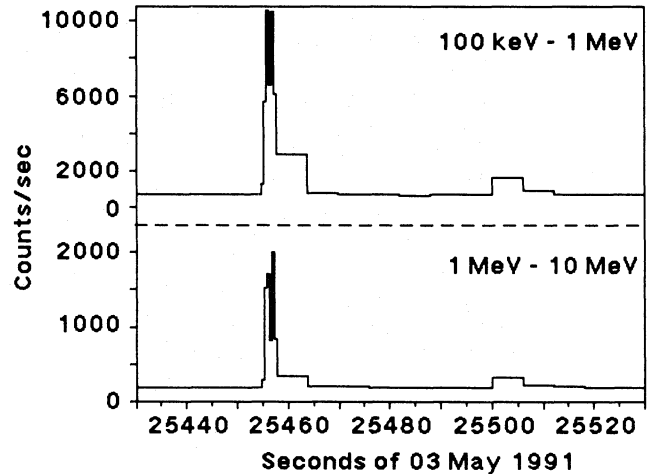


Fig. 3. Lightcurves obtained from the COMPTEL burst detectors. Top: 0.1 MeV - 1 MeV, bottom: 1 MeV - 10 MeV.

At the onset of the burst, the BATSE instrument on board GRO triggered the COMPTEL burst detectors, which subsequently accumulated a time sequence of spectra in "Single Detector Mode". The deadtime corrected and energy calibrated lightcurves from these burst detectors are shown in Fig. 3. GRB 910503 consists of a main pulse with sub-second substructure followed by a second small pulse 45 s after burst onset. The total duration of the burst is ~ 60 s. It may be concluded from Figs. 2 and 3 that (i) the "interpulse" region does not contain significant emission from the source, and, (ii) that the contribution from background radiation is small, at least during the first pulse.

Inspection of the lightcurves obtained from the low and high range burst detectors (Fig. 3) indicates significant differences in the shapes of these two lightcurves. We have calculated hardness ratios

$$H = \frac{\sum_{high}}{\sum_{low}} \quad (2)$$

where Σ_{high} and Σ_{low} is the sum of background subtracted and deadtime corrected counts in the (high) 1 MeV - 10 MeV range and (low) 0.1 MeV - 1 MeV range respectively. Both pulses including the two subpulses of the first pulse show a significant hard-to-soft evolution during the burst event (Fig. 4). This is similar to earlier SMM results reported by Norris et al. (1986), that a hard-to-soft evolution is a characteristic for bursts with pulses of ≥ 1 s duration. Attempts to investigate the telescope

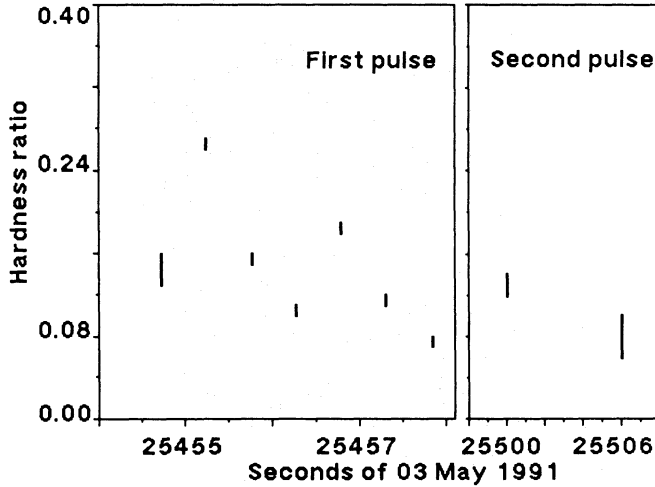


Fig. 4. Hardness ratio for both pulses of GRB 910503

event lightcurve in order to search for periodicities, as reported recently by the Ulysses team (Boer et al. 1991), are in progress. However, the data gaps in the first and, to a lesser extent, in the second pulse due to telemetry deadtime effects in the instrument complicate this analysis.

3.2. Energy spectra and fluence

Figure 5 shows the energy spectrum for each pulse as derived from telescope events. GRB 910503 is a hard event with significant emission up to ~ 10 MeV. In order to fit the energy spectrum of events observed in the imaging "Double Scatter Mode" we first simulated photon spectra at the proper burst location (see below) in order to determine the instrument response. This simulated response - derived from photon interactions in a COMPTEL mass model - was then used to determine the burst photon spectrum from the observed count spectrum. The best fit was achieved by fitting the count spectrum to a power-law folded through the simulated response. Maximum likelihood statistics (rather than χ^2) were used due to the low number of observed counts. Selecting 10 s of observed events from each pulse, using standard time-of-flight and pulse shape event selection windows and accepting all events from within $\pm 15^\circ$ around the burst position, we obtained the following power-law indices for best fit photon spectra (Fig. 5): first pulse: $\alpha = -1.97 \pm 0.44(1\sigma)$, second pulse: $\alpha = -1.99 \pm 0.49(1\sigma)$.

The energy loss spectra obtained from the single burst detectors are shown in Figure 6. Six consecutive spectra and the first of the tail spectra (9 s total integration time) have been added and background subtracted. These spectra contain the first pulse including most of the emission as seen by the burst detectors (see Fig. 3). Preliminary results were obtained by comparing the count spectrum in each range (Fig. 6) with a simulated count spectrum produced by a model power-law

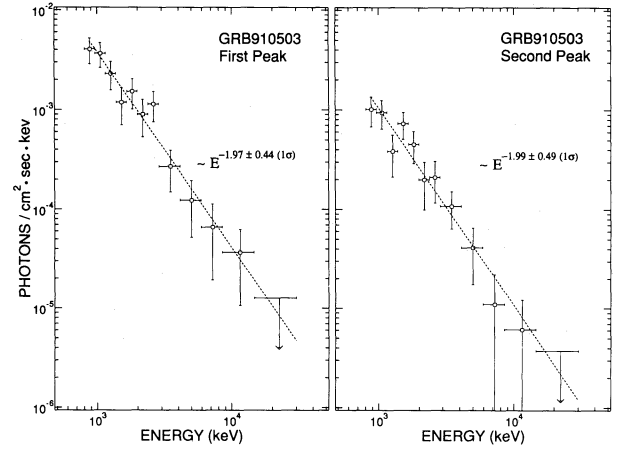


Fig. 5. Best fit telescope event spectra for first pulse (25454 s - 25464 s) and second pulse (25500 s - 25510 s).

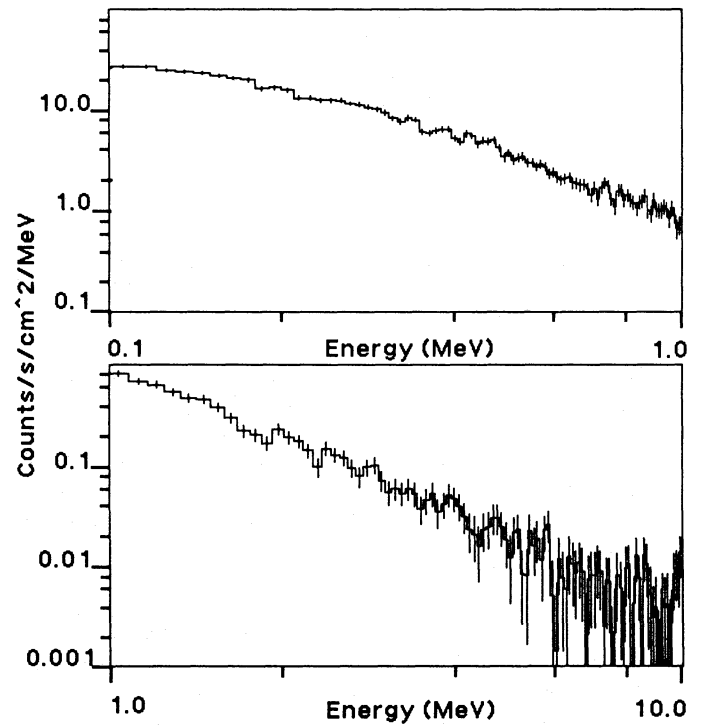


Fig. 6. Background subtracted count spectra for first pulse (top: low range, bottom: high range) obtained from COMPTEL's burst detectors.

photon spectrum injected at the burst incident direction into the COMPTEL mass model. Various power-law spectra in the range $E^{-1.7}$ to $E^{-2.3}$ were tested. Good agreement was obtained, again, for a $E^{-2.0}$ input spectrum consistent with the results from the telescope event spectrum.

Using energy integrated single detector count rates obtained during both pulses (Fig. 3) we estimate the burst fluence to be $S(> 0.1 \text{ MeV}) \sim 2 \times 10^{-4} \text{ erg/cm}^2$ and $S(> 1.0 \text{ MeV}) \sim 7 \times 10^{-5} \text{ erg/cm}^2$. This is in good agreement with the fluence estimate derived from the telescope event photon spectrum (Fig. 5) which gives $S(> 0.8 \text{ MeV}) = (8.6 \pm 1.5) \times 10^{-5} \text{ erg/cm}^2$.

3.3. Location

A simple illustration of the working principles of COMPTEL is shown in Figure 7. As described earlier, each photon, detected by COMPTEL, produces an event circle of radius ϕ (Fig. 1). The common celestial source position of these photons, corresponding to totally absorbed events, can therefore be described by the intersection of all circles. Using events obtained during the first four seconds of the event (note that a subset was selected for demonstration purposes only), it is clear (Fig.7) that the event circles have a unique intersection: the GRB 910503 position is located near the galactic anticentre. In order to accurately map the sky region around GRB

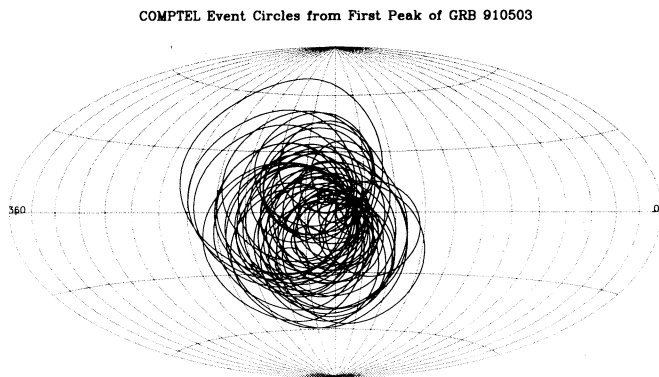


Fig. 7. Demonstration of the COMPTEL imaging principle using the intersection of source "event circles". The source position is near the galactic anticentre.

910503, we have used independent image restoration methods. In general, these methods make use of the instrument point spread function (PSF) and test distributions in the data space (photon scatter direction and scatter angle) for any source signatures. The maximum entropy method (e.g. Gull and Skilling 1984) searches for the "sky" which, after convolution with the telescope response, produces the flattest solution (source distribution) consistent with the given data and response function. Details on application of the maximum entropy method applied to COMPTEL data can be found in Diehl and Strong (1987) and Strong et al. (1991). The application of the maximum likelihood method to COMPTEL data (de Boer et al. 1991) compares a model input sky, again convolved with the instrument response, with the observed data. A third method has been employed which is independent of instrument response and basically consists of an empirical study of the distribution of the event scatter angles relative to various test source positions.

The results of the maximum entropy method applied to GRB 910503 are shown in Figure 8. We have selected 193 source events (1 -20 MeV) obtained between 25453 s - 25510 s (both pulses, Fig.2). The number of background events during 57 s is estimated to be about 30, using preliminary deadtime analysis. The telescope response used in this analysis is based on measurements of the full response for a number of known calibration sources and assuming a E^{-2} spectrum. The presence of a point source is clearly indicated. The centre of the contour map is at about $(l,b) = (171.5^\circ, 6.0^\circ)$. In order to determine the most likely position with its corresponding errors, the maximum likelihood method was applied resulting in a burst

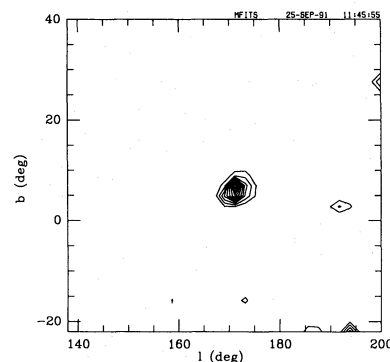


Fig. 8. Maximum entropy skymap of the GRB 910503 burst region. The contours are given in relative flux units.

position of $(l,b) = (171.8^\circ, 6.4^\circ)$ with a 99% (2.6σ) statistical confidence radius of about 2° . The result is slightly dependent on the applied data selections. Due to the fact that this burst, being 31° off the telescope line-of-sight, is located near the edge of the COMPTEL field-of-view, a systematic error of up to 1° can not be excluded. Finally, the third method which tests the distribution of event scatter angles gives a position at $(l,b) = (171^\circ, 7^\circ)$, consistent with the previous methods. A comparison with locations obtained from "triangulations" of event arrival times using data from other spacecraft has been successful and details of this and the investigation of the error box to search for counterparts at other wavelengths will be discussed in a forthcoming paper.

4. Conclusions

The cosmic gamma-ray burst GRB 910503, so far the strongest of the bursts observed by COMPTEL in its field of view, is a "classical" hard transient, located near the galactic anticentre with significant emission up to several MeV. *For the first time a direct MeV image of a cosmic gamma-ray burst has been obtained.* It has been demonstrated that COMPTEL, the first imaging Compton telescope operational in space, has unique imaging capabilities in the largely unexplored 1 - 30 MeV energy band. Independent spectral data demonstrate that spectral evolution has been detected during both pulses indicating a softening of the nonthermal particle energy distribution on time scales of a few seconds.

References

- Boer, M. et al., 1991, 22. ICRC, OG 2.3, preprint
- de Boer, H. et al., 1991, Data Analysis in Astronomy IV, in press
- Diehl, R., Strong, A.W., 1987, Data Analysis in Astronomy III, Plenum, New York, 55
- Gull, S.F., Skilling, J., 1984, IEEE Proc. 131, 646
- Norris, J.P. et al., 1986, ApJ 301, 213
- Schönfelder, V. et al., 1984, IEEE Trans. Nucl. Sci. NS-31,766
- Strong, A.W. et al., 1991, Data Analysis in Astronomy IV, in press
- Winkler, C. et al., 1986, Adv. Space Res. 6, No.4, 113

This article was processed by the author using Springer-Verlag L^AT_EX A&A style file 1990.